Int. J. Heat Mass Transfer. Vol. 29, No. 6, pp. 869–877, 1986
Printed in Great Britain

0017–9310/86 $3.00 + 0.00
Pergamon Journals Ltd.

Numerical predictions of natural convection in a Trombe wall system

S. J. ORMISTON,† G. D. RAITHBY and K. G. T. HOLLANDS
Department of Mechanical Engineering, University of Waterloo, Waterloo, Ontario, Canada N2L 3G1

(*Received* 6 *March* 1985 *and in final form* 25 *November* 1985)

Abstract— In a Trombe wall passive heating system, air from a room is circulated by natural convection through a narrow channel formed by a window on one side and a wall on the other. The circulating flow delivers the solar energy collected by the wall and window to the room. The present paper analyses an idealized Trombe wall system in which the flow is laminar and two-dimensional and the window and wall are isothermal. A dimensional analysis shows that, for a given geometry, the flow and heat transfer are characterized by two Rayleigh numbers. Flow and heat transfer predictions over a wide range of operating conditions were performed using a finite-volume method. These predictions are believed to be the first that fully account for the interaction between the room and channel, and which include the important case where the window temperature is lower than the room temperature.

INTRODUCTION

CONSIDERABLE interest has been shown recently in the application of the Trombe wall, indirect gain, passive solar heating system [1]. In this system a high thermal capacitance wall is located on the room side of large windows, forming a narrow channel between wall and window. Solar energy is absorbed and stored by the wall. Heat is delivered to the adjacent room partly by conduction through the wall and partly by a natural convection flow, through the channel, that is controlled by vents at the bottom and top of the wall.

There are two categories of studies associated with the heat transfer and fluid flow of this system. The first is concerned with natural convection between heated, vertical, parallel plates (simulating the channel region). The other studies are concerned specifically with the Trombe wall system.

In the first of these categories, very significant experimental and theoretical work was reported by Elenbaas [2]. Siegel and Norris [3], Novotny [4], and Aung *et al.* [5] also provided extensive experimental data on the flow and heat transfer between parallel plates. A theoretical study by Aung [6] provided the fully developed solutions for asymmetrically heated, parallel plates. The effect of the inlet pressure condition was studied by Quintiere and Mueller [7]. Bodia and Osterle [8] reported the first numerical study of flow between symmetrically heated, vertical plates. Approximations were introduced which permitted the solution to be marched from the inlet to the outlet (parabolic flow). Aung *et al.* [5] and Miyataka *et al.* [9–11] extended this type of calculation to include asymmetrically heated plates. Aihara [12] concluded that the effect of inlet pressure drop, associated with the acceleration of the fluid entering the parallel plate channel, should be included in the parabolic analyses. The only fully elliptic numerical analyses of the parallel plate problem that include the inlet flow effects were limited to isothermal plates of equal temperature [13, 14]. These showed that the uniform temperature, velocity and pressure at the duct inlet, assumed in the parabolic flow analyses, are unrealistic and indeed affect the predicted heat transfer.

The second category of studies reviewed here are those directly concerned with the Trombe wall problem. Casperson [15] reported results of a preliminary experimental study of a Trombe wall system. Mussulman *et al.* [16–18] provided detailed measurements, numerical predictions and flow visualization results for a system that used silicone oil as the convecting medium. Tichy [19] analysed the effects of inlet and exit losses from the channel, and Akbari and Borgers [20] extended Aihara's work [12] to the Trombe wall problem. Pratt and Karaki [21] solved the boundary layers within a vertical plate channel with asymmetric wall temperatures. More recently [22], they reported solutions for parabolic turbulent flow from an analysis which used an eddy viscosity turbulence model and in which effects of inlet and outlet losses were incorporated. Experimental data for a full size Trombe wall were recently reported by Akbarzadeh *et al.* [23].

The above survey indicates that flow in the full Trombe wall system, including the channel, the room and inlet and outlet sections, has never been predicted. Furthermore, no predictions have been reported for cases in which the window temperature is lower than the room temperature, despite the expected frequent occurrence of this condition. The present study predicts the flow and heat transfer in the entire system, and includes the case where the window temperature is lower than the room temperature. In addition, the results of an analysis is presented which shows that, for

† Present address: Department of Mechanical Engineering, University of Manitoba, Winnipeg, Manitoba, Canada.

NOMENCLATURE

C	clearance above and below wall, Fig. 1 [m]
d	room width, Fig. 1 [m]
g	gravitational acceleration [m s^{-2}]
H	wall height, Fig. 1 [m]
k	thermal conductivity of air
l, m	dimensions associated with isothermal region in room, Fig. 1
M^*	dimensionless mass flow through channel, equation (8)
Nu_1	Nusselt number for wall, equation (6)
Pr	Prandtl number of air, (γ/α)
Q_1	total rate of heat transfer from wall to air in channel, Fig. 1
Q_2	total rate of heat transfer from window to air in channel, Fig. 1
Q_R	total heat delivered to room $(Q_R = Q_1 + Q_2)$
Ra_E	Rayleigh number, equation (5)
Ra_I	Rayleigh number, equation (4)
S	spacing between window and wall, Fig. 1
T_1	wall temperature, Fig. 1
T_2	window temperature, Fig. 1
T_3	'room' temperature, Fig. 1
$\bar{T}$	average channel wall temperature, $(T_1 + T_2)/2$
$\bar{v}$	average air velocity along channel [m s^{-1}]
v_{ref}	reference velocity, equation (3)
W	width of wall, Fig. 1.

Greek symbols

ν	kinematic viscosity of air [m^2 s^{-1}]
α	thermal diffusivity of air [m^2 s^{-1}].

a given geometry, the flow and heat transfer is defined by two Rayleigh numbers. The combined results of the present study improves both the understanding and predictive capabilities related to the flow and heat transfer in Trombe wall systems.

PROBLEM DESCRIPTION

Description of idealized problem

The idealized Trombe wall problem considered in this study is shown in Fig. 1. Radiation through the 'window' on the left side of the room heats the surface of the 'Trombe wall' that faces the window to a uniform temperature T_1. For the purposes of the present study, the top, bottom, and room-side surfaces of the wall were taken to be adiabatic. The window temperature was assumed isothermal at temperature T_2, where $T_2 \leqslant T_1$. Air is drawn by natural convection through the clearance of width C below the wall, along the channel of spacing S between the wall and window, and is discharged through the clearance C between the top of the wall and the ceiling. The flow delivers heat to the room and, being cooled, is circulated back through the channel.

The heat transfer within the room is a complex process that, in applications, will involve heat exchange with the walls, interaction with the air circulation system, the effect of heat sources in the room, etc. In the present model, the natural convection flow was assumed to move everywhere freely through the room, but the temperature of the air within the trapezoidal region indicated in Fig. 1 was enforced to be T_3. This models the case where the room walls are adiabatic but a perfect heat exchanger (infinite heat transfer coefficient and zero pressure loss) maintains the T_3 temperature.

In the present study, the geometry was defined by the following lengths, expressed in terms of the channel spacing S,

$$H = 18S, \quad C = S, \quad W = S, \quad d = 20S. \tag{1}$$

The room therefore has a square cross-section, and has identical clearances between the wall and the floor, window and ceiling. The heat load delivery area is defined by

$$l = 11S, \quad m = 5S. \tag{2}$$

Dimensionless parameters

The full equations of motion, valid for laminar or turbulent flow, are used as the starting point in an

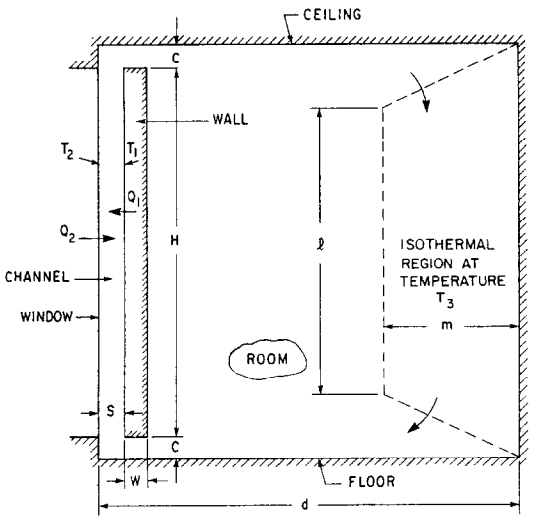

FIG. 1. Schematic for the idealized Trombe wall problem studied. Cross hatched sections denote adiabatic surfaces.

analysis to determine the important dimensionless groups governing the flow and heat transfer in the idealized problem just described. These equations are simplified by asserting that the mean flow is two-dimensional, the fluid is Newtonian, and the Boussinesq approximation applies. These equations are then non-dimensionalized [24] using reference length l_{ref}, time t_{ref}, velocity v_{ref} [25], pressure p_{ref} and temperature ΔT_{ref}, where

$$l_{ref} = S, \quad \Delta T_{ref} = (T_1 - T_3), \quad v_{ref} = \sqrt{\frac{g\beta \Delta T_{ref} S}{1+Pr}}$$
$$t_{ref} = \frac{l_{ref}}{v_{ref}}, \quad p_{ref} = \rho v_{ref}^2. \tag{3}$$

Upon simplification, the non-dimensional equations of motion and boundary conditions are found to contain the length ratios defined by equations (1) and (2)—i.e. H/S, C/S, etc.—as well as Prandtl number, Pr, and the following two Rayleigh numbers

$$Ra_I = \frac{g\beta(T_1 - T_2)S^3}{\nu\alpha} \tag{4}$$

$$Ra_E = \frac{g\beta(\bar{T} - T_3)S^4}{\nu\alpha H}; \quad \bar{T} = \frac{T_1 + T_2}{2}. \tag{5}$$

The 'internal' Rayleigh number, Ra_I, governs the natural convection interaction between the wall and window. The 'external' Rayleigh number, Ra_E, governs the natural convection interaction between the room and the channel. If $Ra_E = 0$, and $Ra_I > 0$, a flow recirculation should occur between the wall and window that is analogous to that in a differentially heated vertical channel, closed at the top and bottom, that has been frequently studied. The other limiting case, $Ra_I = 0$, $Ra_E > 0$, is identical to the problem of natural convection flow between isothermal symmetrically heated plates in an infinite environment, except for the inlet and outlet effects.

In Trombe wall applications, the working fluid is air (so $Pr = 0.71$), $Ra_I \lesssim 10^7$, and $Ra_E \lesssim 10^5$. The present study is limited to $0 \leqslant Ra_I \leqslant 10^5$, and $0 \leqslant Ra_E \leqslant 10^5$ where the flow is presumed to be laminar. The limitation on the Ra_I range covered by the analysis is therefore quite restrictive, but the results do provide quantitative data for a portion of the parameter range of interest and insight into the expected flow behaviour.

The total natural convection heat transfer *from* the Trombe wall and window to the fluid in the channel are respectively Q_1 and Q_2 so that the heat delivered to the room is $Q_R = (Q_1 + Q_2)$. The heat flow Q_1 is expressed non-dimensionally in terms of a Nusselt number as

$$Nu_1 = \frac{Q_1 S}{(T_1 - T_3)Hk}. \tag{6}$$

A knowledge of Nu_1 permits Q_1 to be calculated. The heat delivered to the room Q_R can be calculated from the ratio

$$\frac{Q_R}{Q_1} = \frac{Q_1 + Q_2}{Q_1} \tag{7}$$

which is a measure of the Trombe wall effectiveness. For the case when the window and wall temperatures are the same, $Q_2 \approx Q_1$, so this ratio should approach a value near 2. As the window temperature drops relative to T_1, the heat flow Q_2 drops and eventually changes sign. At the point where $(T_1 + T_2)/2 = T_3$, $Q_2 \approx -Q_1$ and the heat delivered to the room is nearly zero. The regime of still lower values of T_2, where there is a net heat loss from the room to the window ($Ra_E < 0$), was not considered in this study.

The ratio Q_2/Q_1 can be obtained directly from equation (7) once Q_R/Q_1 is specified. Another quantity of interest is Q_{1-R}/Q_1, the ratio of the net heat flow from the wall delivered to the room to the total heat transferred from the wall. Predicted values of both Q_R/Q_1 and Q_{1-R}/Q_1 will be presented in this paper.

The mass flow induced through the channel is also of interest. This can be calculated from the dimensionless mass flow rates, M^*, that are also reported below. M^* is defined as follows:

$$M^* = \bar{v}/v_{ref} = Re\sqrt{\frac{Pr(1+Pr)}{(HRa_E/S + \frac{1}{2}Ra_I)}}. \tag{8}$$

In equation (8), $\bar{v}$ is the average velocity across the channel and the Reynolds number is defined as $Re = \rho S\bar{v}/\mu$.

MATHEMATICAL FORMULATION AND SOLUTION

As already stated, the flow is assumed to be laminar, Newtonian and two-dimensional, and the Boussinesq approximations are applied; the geometry is shown in Fig. 1. The appropriate form of the equations of motion depends on the type of computational grid and on the particular discrete method used. This section therefore first describes the grid, then the equations of motion, and finally briefly describes the solution technique used.

Computational grid

The computational grid, shown in Fig. 2, was orthogonal with one co-ordinate (constant x_2) forming closed paths that wrap around the wall. The plotter used to generate Fig. 2 displayed discontinuities in the grid-line slopes but in reality the grid was smooth and it subdivided the domain into areas which, except at the corners of the solution domain, were fully orthogonal. This grid was generated using a package developed by Karpik [26], which utilizes a refinement of the method proposed by Barfield [27].

The flow and heat transfer results reported below were obtained using 1600 control volumes, 20 in the x_2-direction by 80 in the x_1-direction in Fig. 2. Of these, 680 control volumes were distributed in channel between the isothermal surfaces, with another 320 in the top and bottom channel and vent regions, and 600 in the room. The density of the grid in the x_2-direction was highest near the wall and window and, in the x_1-direction, near the bottom and top of the channel.

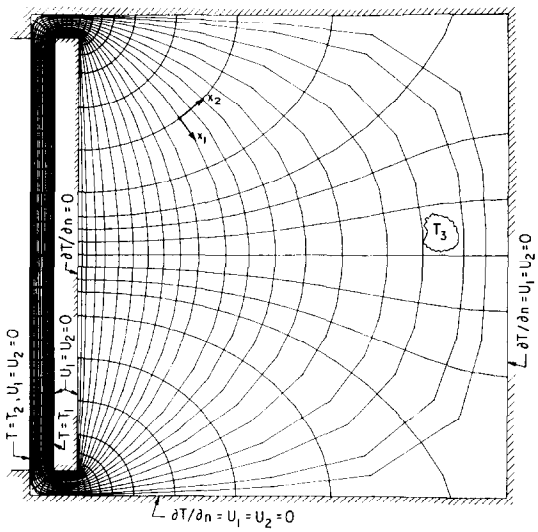

FIG. 2. Computational grid used for the predictions reported. Boundary conditions on the solid surfaces are also shown.

Equations of motion

The equations of mass, momentum and energy conservation written in general orthogonal coordinates, simplified by incorporating the approximations outlined above are [28]

$$\frac{\partial}{\partial x_1}(\rho h_2 u_1)+\frac{\partial}{\partial x_2}(\rho h_1 u_2)=0 \tag{9}$$

$$\frac{\partial}{\partial t}(\rho u_1)+\frac{1}{h_1 h_2}\left[\frac{\partial}{\partial x_1}(\rho h_2 u_1 u_1)+\frac{\partial}{\partial x_2}(\rho h_1 u_2 u_1)\right] = -\frac{1}{h_1}\frac{\partial p}{\partial x_1}+\frac{1}{h_1 h_2}\left[\frac{\partial}{\partial x_1}(h_2\sigma_{11}) + \frac{\partial}{\partial x_2}(h_1\sigma_{12})\right]+\left(\frac{\sigma_{12}-\rho u_1 u_2}{r_1}\right) -\left(\frac{\sigma_{22}-\rho u_2^2}{r_2}\right)-\rho\beta g_1(T-T_\infty) \tag{10}$$

$$\frac{\partial}{\partial t}(\rho u_2)+\frac{1}{h_1 h_2}\left[\frac{\partial}{\partial x_1}(\rho h_2 u_1 u_2)+\frac{\partial}{\partial x_2}(\rho h_1 u_2 u_2)\right] = -\frac{1}{h_2}\frac{\partial p}{\partial x_2}+\frac{1}{h_1 h_2}\left[\frac{\partial}{\partial x_1}(h_2\sigma_{12}) + \frac{\partial}{\partial x_2}(h_1\sigma_{22})\right]+\left(\frac{\sigma_{12}-\rho u_1 u_2}{r_2}\right) -\left(\frac{\sigma_{11}-\rho u_1^2}{r_1}\right)-\rho\beta g_2(T-T_\infty) \tag{11}$$

$$\frac{\partial}{\partial t}(\rho T)+\frac{1}{h_1 h_2}\left[\frac{\partial}{\partial x_1}(\rho h_2 u_1 T)+\frac{\partial}{\partial x_2}(\rho h_1 u_2 T)\right] = -\frac{1}{h_1 h_2}\left[\frac{\partial}{\partial x_1}(h_2 q_1)+\frac{\partial}{\partial x_2}(h_1 q_2)\right] \tag{12}$$

where

$$q_1=-\frac{k}{C_p h_1}\frac{\partial T}{\partial x_1} \qquad q_2=-\frac{k}{C_p h_2}\frac{\partial T}{\partial x_2}$$

$$\sigma_{11}=2\mu\left[\frac{\partial u_1}{h_1\,\partial x_1}+\frac{u_2}{r_1}\right] \tag{13}$$

$$\sigma_{12}=\mu\left[\frac{\partial u_1}{h_2\,\partial x_2}+\frac{\partial u_2}{h_1\,\partial x_1}-\left(\frac{u_1}{r_1}+\frac{u_2}{r_2}\right)\right]$$

$$\sigma_{22}=2\mu\left[\frac{\partial u_2}{h_2\,\partial x_2}+\frac{u_1}{r_2}\right] \tag{14}$$

$$\frac{1}{r_1}=\frac{1}{h_1 h_2}\frac{\partial h_1}{\partial x_2} \qquad \frac{1}{r_2}=\frac{1}{h_1 h_2}\frac{\partial h_2}{\partial x_1}. \tag{15}$$

In these equations u_1 and u_2 are the orthogonal velocities in the x_1- and x_2-directions, respectively, T is temperature, σ is stress and r is grid curvature. The 'buoyancy term' in the x_i-direction is $-\rho\beta g_i(T-T_\infty)$ where g_i is the component of gravity in the direction of x_i. The predicted velocities and temperatures must be independent of the reference temperature T_∞ chosen, but it is convenient to select T_∞ as the room temperature T_3. All property values in equations (9)–(14) were treated as constant.

The values of u_1 and u_2 on all solid boundaries in Fig. 1 were prescribed as zero. The heat flux was set to zero on the cross hatched boundaries in the figure, T_1 and T_2 were prescribed on the wall and window respectively, and T_3 was enforced over the 'heat exchanger' region in Fig. 1.

Solution method

A finite-volume method, similar to the method described by Patankar [29] for the special case of Cartesian grids, was used to solve the general orthogonal equations. Details are provided by Raithby *et al.* [28] and in the thesis of Ormiston [24].

The 'outer' interation loop in the solution algorithm began by updating the coefficients of the linear algebraic equations representing mass, momentum and energy. At the completion of one outer iteration, the solution to these equations was obtained to some tolerance. The loop was repeated until the following convergence criterion was met

$$\frac{\Delta\phi_{\max}}{D(\phi)}\leqslant\varepsilon^{\phi}$$

where ϕ is a dependent variable, $\Delta\phi_{\max}$ is the maximum change in ϕ from one coefficient update to the next, and $D(\phi)$ is the difference between the maximum and minimum values of ϕ within the solution domain. In most cases, the temperature and pressure were driven to $\varepsilon^{T}=\varepsilon^{p}\leqslant 0.0005$ but in a few cases a mild oscillatory behaviour resulted in an intermittent exchange of fluid from the channel to the room. By plotting the wall heat fluxes in these cases over a number of oscillations, it was established that the amplitudes of the variations in Q_1 and Q_2 were insignificant compared to Q_1 and Q_2, respectively.

Calculations were performed on an IBM4341 computer, with CPU times of approximately 70 min for each solution.

Code verification runs

Before attempting to solve the Trombe wall problem the code was extensively exercised on a number of problems to check its validity. Calculations were performed for the classical Cartesian problems of flow in a square cavity driven by a sliding lid, and for natural convection in a square cavity with differentially heated walls. Forced flow through a tank [30] was also solved. The predictions were found to agree exactly with those from an independently developed code. Next, natural convection and Couette flow in a cylindrical annulus were analysed using a circular cylinder coordinate system, and these were again checked by comparisons respectively with prior calculations and with the exact solution.

The problem of natural convection between parallel, symmetrically heated, vertical plates in an infinite environment was solved and the results compared to the parabolic-flow predictions of Worku [31]. Excellent agreement was found for both temperature and velocity except very near the inlet. Mesh refinement in this region established that the present calculations were very nearly grid independent. The small discrepancies were concluded to arise from the elliptic nature of the flow near the inlet, which was not accounted for in Worku's analysis. The inlet flow to vertical, parallel, symmetrically heated plates was also predicted and results compared with the predictions of Kettleborough [13] and Nakamura *et al.* [14]. These two previous studies were in substantial disagreement with each other; the present results [24] fell much closer to those of Nakamura *et al.*, but significant differences did exist.

Based on the above, and other studies, it was concluded that the code could be reliably applied to the Trombe wall problem. Results for this problem are now presented.

RESULTS FOR TROMBE WALL PROBLEM

The average heat transfer rates are the quantities of design interest, so that these are presented first. Some details of the flows that give rise to these results will be presented later.

Average heat transfer predictions

$\mathrm{Ra}_E = 0$, $\mathrm{Ra}_I > 0$. It is instructive to first discuss results for $Ra_E = 0$, $Ra_I \geqslant 0$. In this limit, the heat transferred from the wall should mainly flow to the window, and a recirculation pattern should be established in the channel with zero net through-flow. The predicted heat transfer would, under these conditions, be expected to agree closely with those for heat transfer across a vertical cavity with adiabatic walls at the top and bottom. A comparison with the predictions of Wong and Raithby [32, 33] indicate that the present heat transfer is within 3% over the entire Ra_I range.

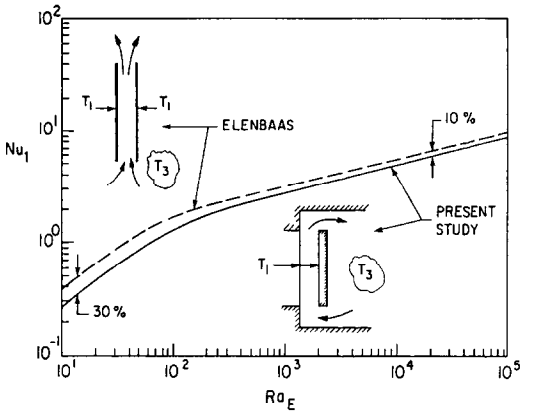

FIG. 3. Comparison of the heat transfer from parallel plates measured by Elenbaas [2] with the predicted heat transfer from the Trombe wall geometry. Losses at the inlet and outlet are thought to account for the discrepancy.

$\mathrm{Ra}_I = 0$, $\mathrm{Ra}_E > 0$. Another limiting case of interest occurs when the wall and window are at the same temperature ($T_1 = T_2$) but the room is cooler. Except for pressure losses and asymmetries, due to entrance and exit effects, this problem resembles the 'parallel, symmetrically heated plates in an infinite environment' problem [2, 8] that has been extensively studied. The predictions of the present study are compared to the edge-corrected measurements of Elenbaas [2] in Fig. 3. The losses appear to cause a 10% reduction in heat transfer at $Ra_E = 10^4$, with the difference increasing to about 30% at $Ra_E = 10$.

Mass flow through channel, $\mathrm{Ra}_I \geqslant 0$, $\mathrm{Ra}_E \geqslant 0$. The dimensional mass flow through the channel increases monotonically with Ra_E, but Fig. 4 shows that the dimensionless mass flow rate through the channel is nearly independent of Ra_E provided Ra_I/Ra_E is sufficiently small. Large values of Ra_I/Ra_E tend to create a counter flow along the cold window which chokes off the flow through the channel.

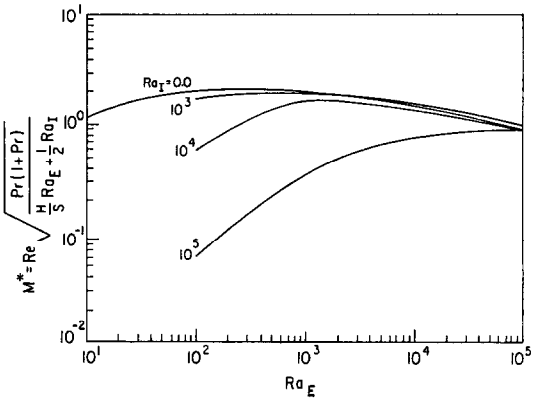

FIG. 4. Dimensionless mass flow through the channel vs external Rayleigh number for $Ra_I = 0$, 10^3, 10^4 and 10^5.

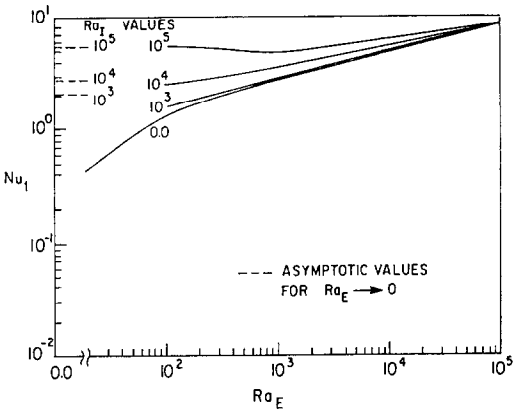

FIG. 5. Dimensionless heat transfer from the Trombe wall vs external Rayleigh number for $Ra_I = 0$, 10^3, 10^4 and 10^5. The asymptotic results for $Re_E \to 0$, are also shown.

Heat transfer from the Trombe wall. The dimensionless heat transferred from the Trombe wall, Nu_1, is plotted in Fig. 5. The $Ra_I = 0$ curve corresponds to the curve compared to the Elenbaas measurements in Fig. 3. For larger Ra_I, the wall heat transfer Q_1 increases because of extra heat losses to the window. In the limit, as $Ra_E \to 0$, the asymptotic value of Nu_1 represents heat transfer mainly between the wall and window, as discussed above. It is interesting to note that Nu_1 passes through a minimum as the $Ra_E \to 0$ asymptote is approached. Figure 5 permits the total heat flow from the wall, Q_1, to be calculated.

Heat transfer to the room and window. Once Q_1 is known, the total heat delivered to the room, $Q_R = Q_1 + Q_2$, can be found from Fig. 6 from ratio Q_R/Q_1. For

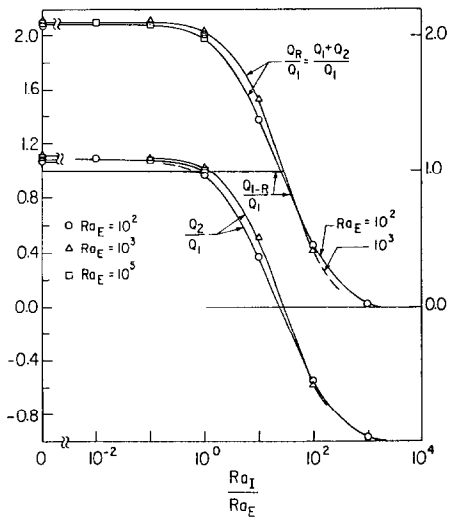

FIG. 6. Plot of the total heat transfer to the room, Q_R, the fraction of the heat transfer from the wall that is delivered to the room, Q_{1-R}, and the heat transfer from the window, Q_2, all normalized by Q_1.

$Ra_I/Ra_E < 1$, the window supplies more heat to the room than the wall (so that Q_R/Q_1 exceeds 2) because of the flow asymmetry already discussed. As Ra_I increases (i.e. the window temperature drops), the heat supplied to the room decreases until at $Ra_I/Ra_E \approx 25$, the net heat transfer from the window is zero. For $Ra_I/Ra_E > 25$, a diminishing fraction of Q_1 is delivered to the room with the remainder being lost to the window.

The heat transfer interaction between the wall, the window and the room is further clarified in Fig. 6 by plotting the ratio Q_2/Q_1, and the fraction of Q_1 delivered to the room (Q_{1-R}/Q_1). Q_2/Q_1 approaches a value of roughly 1.1 for $T_1 = T_2$ and falls to -1 for high values of Ra_I. Over the regime of positive Q_2, all the heat transferred from the wall is delivered to the room. The fraction of Q_1 delivered to the room when Q_2 is negative coincides with the Q_R/Q_1 curves discussed in the previous paragraph. At $Ra_I/Ra_E \gtrsim 400$, less than 10% of the heat transferred from the wall is delivered to the room.

Window temperatures will be encountered in practice that are sufficiently cold that $\bar{T} - T_3$ becomes negative. In such cases, the net flow through the channel will reverse and the Trombe wall system will deliver heat from the room to the wall and window ($Q_R < 0$). Under such conditions, the circulation should be eliminated by closing the vents.

Velocity and temperature distributions

With the overall performance of the system understood, it may be of interest to examine briefly some of the details of the flow that give rise to the performance just reported.

$Ra_E \gg Ra_I$. Figures 7A and B present streamline and isotherm plots respectively for $Ra_I = 0$, $Ra_E = 10^5$. The heated wall and window induce a channel flow that results in a general clockwise circulation in the room. The flow drawn into the channel separates near the bottom of the wall causing higher velocities to occur near the window. This results in the asymmetric isotherms in Fig. 7B. This figure also indicates that significant stratification occurs near the ceiling in the room. An examination of the isobars [24] indicates significant variations in pressure across the channel near the inlet and outlet of the channel, bringing into question the validity of the parabolic flow approximation for this problem.

$Ra_E \ll Ra_I$. Figures 7C and D present streamline and isotherm plots respectively for $Ra_I = 10^4$, $Ra_E = 10^2$. The flow in this case primarily circulates within the slot with very little exchange with the room. A slightly unsteady oscillation, discussed previously, results in the small eddies shed from the channel. The isotherms in Fig. 7D show that a strong stratification develops along both the floor and ceiling.

Other cases. Figures 7A, B and C, D illustrate flow patterns dominated respectively by Ra_E and Ra_I. For cases where $Ra_E \approx Ra_I$, the flow moves down along the cold window but separates before reaching the bottom

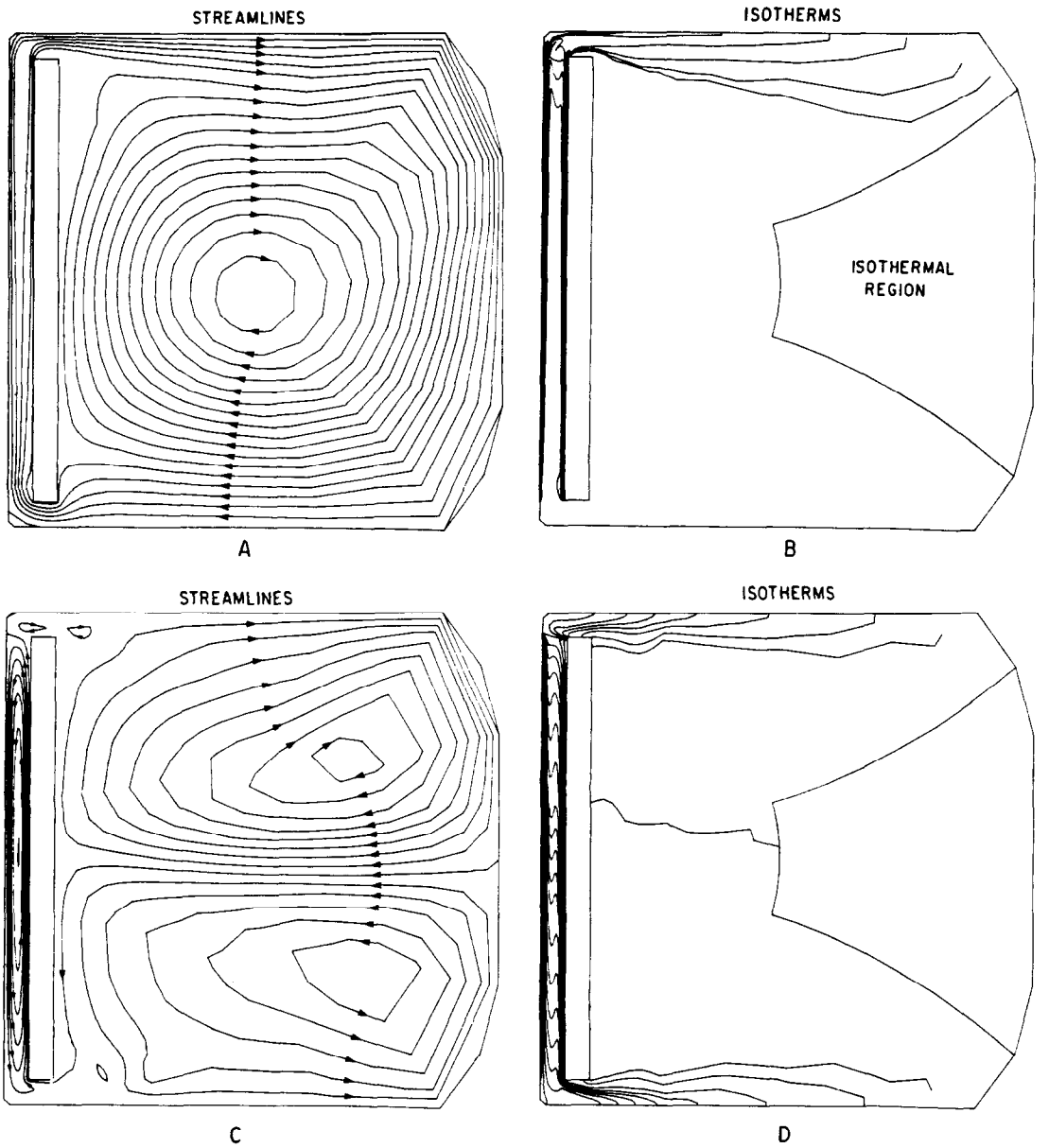

FIG. 7. Streamlines (A) and isotherms (B) for $Ra_E/Ra_I \gg 1$ ($Ra_I = 0, Ra_E = 10^5$). Streamlines (C) and isotherms (D) for $Ra_E/Ra_I \ll 1$ ($Ra_I = 10^5$, $Ra_E = 10^2$).

because of the channel through flow. This and other cases have been presented by Ormiston [24].

DISCUSSION

The results presented in this paper represent the first calculations of two-dimensional, laminar, fully elliptic flow in a Trombe wall system. The contributions of this study included the following:

1. A non-dimensionalization of the equations of motion resulted in the conclusion that the main parameters governing the flow and heat transfer, for a given geometry, are the internal and external Rayleigh numbers, Ra_I and Ra_E. The flow and heat transfer in the Trombe wall in limiting cases, where $Ra_I \gg Ra_E$ and $Ra_I \ll Ra_E$ closely resemble those for two classical natural convection problems.
2. The paper presents the first Trombe wall predictions which fully account for the interaction of the room and the flow within the channel, and which examine the important cases where the window temperature is lower than the room temperature.
3. Heat transfer results have been presented for determining the efficiency by which heat stored in the wall is delivered to the room. Predicted mass flow rates through the channel are also presented.
4. A survey of the local velocities and temperatures provide further insight into the behaviour of the

system. Pressure predictions indicate significant pressure variations across the channel near the inlet and outlet, bringing into question the validity of parabolic solution procedures.

Acknowledgements—The authors are grateful for assistance from S. Karpik, P. Galpin, J. Van Doormaal, and other members of the Computational Fluid Dynamics Group. The work was supported by the Natural Science and Engineering Research Council of Canada.

REFERENCES

1. D. Carriere, *Solar Houses for a Cold Climate*. Scribner, New York (1980).
2. W. Elenbaas, Heat dissipation of parallel plates by free convection, *Physica* **9**, 1–28 (1942).
3. R. Seigel and R. H. Norris, Tests of free convection in a partially enclosed space between two heated vertical plates, *Trans. Am. Soc. mech. Engrs* **79**, 663–673 (1957).
4. J. L. Novotny, Laminar free convection between finite vertical parallel plates. In *Progress in Heat and Mass Transfer* (Edited by T. F. Irvine, Jr.), Vol. 2, pp. 13–22 Pergamon Press, New York (1969).
5. W. Aung, L. S. Fletcher and V. Sernas, Developing laminar free convection between vertical flat plates with asymmetric heating, *Int. J. Heat Mass Transfer* **15**, 2293–2308 (1972).
6. W. Aung, Fully developed laminar free convection between vertical plates heated asymmetrically, *Int. J. Heat Mass Transfer* **15**, 1577–1580 (1972).
7. J. Quintiere and W. K. Mueller, An analysis of laminar free and forced convection between finite vertical parallel plates. Paper presented at the Winter Annual Meeting of the ASME, New York (November 1972).
8. J. R. Bodoia and J. F. Osterle, The development of free convection between heated vertical plates, *Trans. Am. Soc. mech. Engrs*, Series C, *J. Heat Transfer* **84**, 40–44 (1962).
9. O. Miyatake and T. Fujii, Free convective heat transfer between vertical parallel plates—one plate isothermally heated and the other thermally insulated, *Kagaku Kogaku* **36**, 405–412 (1972).
10. O. Miyatake, T. Fujii, M. Fujii and H. Tanaka, Natural convective heat transfer between vertical parallel plates—one plate with a uniform heat flux and the other thermally insulated, *Kagaku Kogaku* **36**, 859–864 (1972).
11. O. Miyatake and T. Fujii, Natural convection heat transfer between vertical parallel plates at unequal uniform temperatures, *Kagaku Kogaku* **37**, 491–496 (1973).
12. T. Aihara, Effects of inlet boundary conditions on numerical solutions of free convection between vertical parallel plates, Report Institute of High Speed Mechanics, Tohoku University, No 258, vol. 28 (1973).
13. C. F. Kettleborough, Transient laminar free convection between heated vertical plates including entrance effects, *Int. J. Heat Mass Transfer* **15**, 883–896 (1972).
14. H. Nakamura, Y. Asako and T. Naitou, Heat transfer by free convection between two parallel flat plates, *Numer. Heat Transfer* **5**, 95–106 (1982).
15. R. L. Casperson, Experimental investigation of the Trombe wall passive solar energy system, *Proc. Third National Passive Solar Conference* (1979).
16. R. E. Stotts, R. O. Warrington and R. L. Mussulman, Simulation and a preliminary comparison of passive solar heating systems, ASME, paper No. 80-HT-17 (1980).
17. R. L. Mussulman, R. O. Warrington and P. C. Lin, Natural convection in a scaled Trombe wall geometry, *Heat Transfer and Thermal Performance in Passive Solar Systems*, DOE Conference 830702-Exc., Chap. II (1983).
18. J.-I. Wu, R. L. Mussulman and R. O. Warrington, Parametric study of heat transfer in a Trombe wall geometry, 22nd National ASME/AIChE Heat Transfer Conference, Niagara Falls (1984).
19. J. A. Tichy, The effect of inlet and exit losses on free convective laminar flow in the Trombe wall channel, *J. Sol. Energy Eng* **105**, 187–193 (1983).
20. H. Akbari and T. R. Borgers, Free convective laminar flow within the Trombe wall channel, *Sol. Energy* **22**, 165–174 (1979).
21. R. G. Pratt and S. Karaki, Natural convection between vertical plates with external frictional losses—application to Trombe walls, *Proc. Third National Passive Solar Conference* (1979).
22. R. G. Pratt and S. Karaki, Boundary layer flow in Trombe wall ducts, ASME paper No. 80-HT-20 (1980).
23. A. Akbarzadeh, W. W. S. Charters and D. A. Lesslie, Thermocirculation characteristics of a Trombe wall passive test cell, *Sol. Energy* **28**, 461–468 (1982).
24. S. J. Ormiston, A numerical study of two-dimensional natural convection in a Trombe wall system including vent and room effects, Department of Mechnical Engineering, University of Waterloo (December 1983).
25. G. D. Raithby and K. G. T. Hollands, Natural convection. In *Handbook of Heat Transfer* (Edited by W. M. Rohsenow, J. P. Hartnett and E. N. Ganic). McGraw-Hill, New York (1985).
26. S. R. Karpik, Department of Mechanical Engineering, University of Waterloo, personal communication (1983).
27. W. D. Barfield, Numerical method for generating curvilinear meshes, *J. Computational Phys.* **5**, 23–33 (1970).
28. G. D. Raithby, P. F. Galpin and J. P. Van Doormaal, Prediction of heat and fluid flow in complex geometries using general orthogonal cordinates, *Numer. Heat Transfer* **9**, 125–142 (1986).
29. S. V. Patankar, *Numerical Heat Transfer and Fluid Flow*. Hemisphere, Washington, DC (1980).
30. G. D. Raithby and G. E. Schneider, Numerical solution of problems in incompressible fluid flow: treatment of the velocity–pressure coupling, *Numer. Heat Transfer* **2**, 417–440 (1979).
31. G. Worku, Developing laminar combined natural and forced convection flow between vertical parallel plates, M.Sc. thesis, Department of Mechanical Engineering, Howard University, Washington, DC (1982).
32. H. H. Wong and G. D. Raithby, Improved finite-difference methods based on a critical evaluation of the approximation error, *Numer. Heat Transfer* **2**, 139–163 (1979).
33. G. D. Raithby and H. H. Wong, Heat transfer by natural convection across vertical air layers, *Numer. Heat Transfer* **4**, 447–457 (1981).

CALCUL NUMERIQUE DE LA CONVECTION NATURELLE DANS UNE PAROI TROMBE

Résumé—Dans un système de chauffage passif à paroi Trombe, l'air venant d'une pièce circule par convection naturelle à travers un canal étroit entre une vitre et un mur. L'écoulement qui circule apporte à la pièce l'énergie solaire collectée par le mur et la vitre. On analyse un système Trombe idéalisé dans lequel l'écoulement est laminaire et bidimensionnel, la vitre et le mur sont isothermes. Une analyse dimensionnelle montre que, pour une geométrie donnée, l'écoulement et le transfert thermique sont caractérisés par deux nombres de Rayleigh. L'écoulement et le transfert thermique pour un large domaine de conditions opératoires sont calculés à partir d'une méthode de volumes finis. Ces résultats sont supposés être les premiers qui tiennent complètement compte de l'interaction entre la pièce et le canal, et qui incluent le cas important où la température de la vitre est plus basse que la température de la pièce.

NUMERISCHE BERECHNUNGEN DER NATÜRLICHEN KONVEKTION IN EINEM TROMBEWANDSYSTEM

Zusammenfassung—In einem passiven Heizungssystem mit einer Trombewand zirkuliert Luft aus einem Raum auf Grund natürlicher Konvektion durch einen schmalen Spalt, der durch ein Fenster und eine Wand gebildet wird. Die zirkulierende Strömung transportiert die Sonnenenergie, die durch das Fenster und die Wand aufgenommen wurde, in den dahinterliegenden Raum. In der vorliegenden Arbeit wird ein idealisiertes Trombewandsystem analysiert. Die Strömung ist laminar und zweidimensional. Fenster und Wand sind isotherme Flächen. Eine Dimensionsanalyse zeigt, daß Strömung und Wärmeübergang bei einer gegebenen Geometrie von zwei Rayleighzahlen bestimmt werden. Strömungs- und Wärmeübergangsberechnungen über einen weiten Bereich der Betriebsbedingungen wurden mit Hilfe eines Finite-Volumina-Verfahrens durchgeführt. Diese Berechnungen sind wohl die ersten, welche die Wechselwirkung zwischen Raum und Spalt vollständig in Betracht ziehen und den wichtigen Fall beinhalten, daß die Temperatur des Fensters geringer ist als die des Raumes.

ЧИСЛЕННОЕ ИССЛЕДОВАНИЕ ЕСТЕСТВЕННОЙ КОНВЕКЦИИ В РАДИАТОРЕ ТРОМБА

Аннотация—При пассивном обогреве радиатором Тромба происходит естественноконвективная циркуляция комнатного воздуха через узкий канал, образованный окном с одной стороны и стенкой с другой. Циркулирующий поток переносит солнечную энергию, аккумулированную стенкой и окном в комнате. Исследуется идеальный радиатор Тромба, когда течение ламинарное и двумерное, а окно и стенка изотермические. Анализ размерностей показывает, что для данной геометрии течение и теплообмен характеризуются двумя числами Рэлея. Течения и теплообмен в широком диапазоне режимных параметров рассчитываются численно методом конечного объема. Представляется, что в расчетах впервые полностью учитывается взаимодействие между комнатой и каналом; кроме того, они включают важный случай, когда температура окна ниже, чем стенки.